Geophysical Research Letters

RESEARCH LETTER
10.1029/2026GL121643

Introducing Regularization Constraints Into Combination of GRACE Monthly Terrestrial Water Storage Changes

Wei You[1], Ke Qian[1], Jiangjun Ran[2], and Pavel Ditmar[3]

[1]Faculty of Geosciences and Engineering, Southwest Jiaotong University, Chengdu, China, [2]Department of Earth and Space Sciences, Southern University of Science and Technology, Shenzhen, China, [3]Department of Geoscience and Remote Sensing, Delft University of Technology, Delft, The Netherlands

Key Points:

- GRACE-based terrestrial water storage (TWS) combined solutions with different regularization constraints were developed
- Accuracy of individual and combined TWS solutions was quantified through comparison with the signal model
- TWS changes were also evaluated by comparing with Caspian Sea level (CSL) changes observed by satellite altimetry

Supporting Information:

Supporting Information may be found in the online version of this article.

Correspondence to:

W. You,
youwei@swjtu.edu.cn

Citation:

You, W., Qian, K., Ran, J., & Ditmar, P. (2026). Introducing regularization constraints into combination of GRACE monthly terrestrial water storage changes. *Geophysical Research Letters*, *53*, e2026GL121643. https://doi.org/10.1029/2026GL121643

Received 12 JAN 2026
Accepted 22 MAR 2026

Author Contributions:

Conceptualization: Wei You, Ke Qian, Jiangjun Ran, Pavel Ditmar
Data curation: Wei You
Formal analysis: Wei You, Pavel Ditmar
Investigation: Wei You
Methodology: Wei You, Ke Qian, Pavel Ditmar
Resources: Wei You
Software: Wei You, Ke Qian
Validation: Wei You, Ke Qian
Visualization: Wei You, Ke Qian
Writing – original draft: Wei You, Ke Qian
Writing – review & editing: Wei You, Jiangjun Ran, Pavel Ditmar

Abstract Gravity Recovery and Climate Experiment (GRACE) observation data processed by various institutions yields somewhat different spherical harmonic solutions, which are further used to derive terrestrial water storage (TWS) changes. Combining TWS solutions from different institutions helps to refine the effective signal while removing noise. This study investigates regularization constraints in the context of TWS fusion to enhance the resulting estimates. The considered constraints are Tikhonov regularization of different orders, as well as minimization of month-to-month year-to-year double differences (MYDD), and triple differences (MYTD). Different accuracy and signal evaluation approaches are implemented for both individual and combined solutions. Compared to individual solutions and unregularized combinations, the regularized TWS combined solutions demonstrate lower noise levels. Among them, the second-order Tikhonov regularization performs slightly better than other constraints, providing lower noise levels. This study offers a novel perspective for exploring GRACE-based TWS combination methodologies.

Plain Language Summary Existing approaches on TWS combination have not considered the inclusion of regularization constraints. Here, based on the hydrological characteristics inherent to TWS, we introduced zeroth-, first-, and second-order Tikhonov regularization, as well as MYDD and MYTD regularization constraints into the TWS combination. By comparing the results with individual and unregularized combined solutions, we quantified the accuracy improvements brought by regularization and evaluated the potential signal deviation it may cause. The results show that, compared to unregularized combined solution, regularized combined solutions improve accuracy by 18%. While regularization does not affect low-frequency signals such as annual and semi-annual components, it does lead to energy loss in the high-frequency components of GRACE solutions. Particularly, MYTD constraint tends to suppress signals in non-integer frequency bands. However, considering that GRACE satellites are not well-suited for capturing high-frequency signals, the impact of regularization on high-frequency components can be considered negligible. Introducing regularization into the model combination offers a new approach to enhancing the performance of TWS combination models.

1. Introduction

The Gravity Recovery and Climate Experiment (GRACE) and its successor GRACE Follow-On (GRACE-FO) missions provided unprecedented insights into temporal Earth's gravity field variations. Those variations are primarily triggered by water mass transport processes, which are the primary focus of many scientific researches based on GRACE data (Landerer et al., 2020; Tapley et al., 2019). The global Earth's gravity field is typically parameterized using a spectral representation based on spherical harmonic coefficients (SHCs). Estimates of those coefficients based on GRACE/GRACE-FO data are distributed as a Level 2 product, which is continuously generated and released by GRACE/GRACE-FO Science Data System (SDS; i.e., the Center for Space Research (CSR; Bettadpur (2018)), Jet Propulsion Laboratory (JPL; Yuan (2018)), and German Research Center for Geosciences (GFZ; Dahle et al. (2019))). Level 2 products are also released by other data processing teams (e.g., Institute of Geodesy at Graz University of Technology (ITSG; Kvas et al. (2019)), Wuhan University (WHU; Zhong et al. (2023)), Huazhong University of Science and Technology (HUST; Zhou et al. (2019))). However, a GRACE/GRACE-FO monthly gravity field solution, represented as a set of SHCs, can hardly be used to investigate water mass transport processes directly without any post processing. The SHCs are usually filtered to reduce high-degree/order errors and then transformed into terrestrial water storage (TWS) estimates in the spatial domain (Kusche, 2007; Kusche et al., 2009; Mu et al., 2017; Prevost et al., 2019; Swenson & Wahr, 2006).

TWS fields from different GRACE/GRACE-FO solutions contain distinct error patterns corresponding to different processing strategies adopted by data processing teams, even if the solutions are post-processed with consistently implemented filters. An effective approach to further reduce the noise levels in TWS fields is to merge solutions from different teams to obtain a combined solution, which typically exhibits lower noise levels compared to each member solution. Sakumura et al. (2014) first proposed to combine multiple GRACE solutions from various institutes and proved effectiveness of this approach for noise level reduction. Jean et al. (2018) investigated this approach further, trying various weighting schemes where the weights were assigned based on the differences between the GRACE solutions involved in the combination. They identified variance component estimation (VCE) as the best combination scheme among those considered. Meyer et al. (2023) further advanced this technique by applying an order-specific filter when determining the weights for SHCs up to degree 90 or 96 (truncated to 90), which resulted in more reasonable weights for each GRACE-FO solution.

In addition to GRACE data fusion in the spectral domain based on unconstrained SHCs, GRACE-derived TWS changes can also be merged in the spatial domain. Yan et al. (2021) merged SHC-inverted and mascon (mass concentration)-derived TWS, weighted by uncertainties from the GTCH (generalized three-cornered hat) method, aiming to reliably and robustly quantify a drought event. Gao et al. (2023) assessed the uncertainties of individual GRACE-derived TWS estimates using GTCH method and then generated a fusion TWS model of enhancing SNR (signal-to-noise ratio) across 142 basins globally.

Previous studies have demonstrated that combining either unconstrained SHCs or filtered TWS estimates effectively reduces errors from GRACE observations and background models, thereby allowing the desirable geophysical signal to be presented more clearly. To further enhance the accuracy of GRACE TWS estimation, we introduce regularization when filtered TWS estimations are combined by using VCE as the weighting scheme. The regularization constraints are designed based on the characteristics of climatic signals embedded in the TWS changes.

Within this study, we apply a method originated from Ditmar (2022) to generate various combined TWS solutions regularized with different types of constraints, which could also estimate the uncertainty of each individual solution through the VCE. We should note that in the previous study, this method was mainly exploited to evaluate accuracy of each individual gravity field model, which was merely used to gravity field model combination. In our research, we mainly focus on the gravity field model combination. This study also explores to what extent the signal caused by TWS changes becomes biased (or attenuated) after introducing regularization and identifies the optimal regularization type. To evaluate the performance of the combined solutions, we analyze and compare the combined and individual solutions by calculating residuals in the open ocean and assessing signal retention in river basins categorized by their areas and climate types. Furthermore, to better assess the individual and combined solutions, we use them to estimate Caspian Sea Level (CSL) changes and compare the results with CSL estimates from satellite altimetry observations.

2. Data

We use time series of GRACE monthly solutions up to 60 degree and order in the time interval from August 2002 to July 2016, including the latest GRACE monthly gravity field models CSR Release 06.1, JPL Release 06.1, and GFZ Release 06.1, as well as ITSG-GRACE2018, WHU-GRACE-GPD01s, and HUST-Grace2024 (https://icgem.gfz-potsdam.de/), which are hereafter referred to as CSR, JPL, GFZ, ITSG, WHU and HUST (Table S1 in Supporting Information S1), respectively. Before conducting the combination experiment, it is necessary to ensure that all the time series consist of the same set of months. For the sake of temporal consistency, solutions for specific months are removed from all the time series when gaps occur in at least one of the time series, resulting in 152 monthly solutions in each time series. Considering the geocentric motion, corresponding degree-one SHCs (Sun et al., 2016) are added to the monthly solutions. Furthermore, $C_{2,0}$ and $C_{3,0}$ terms are replaced by those from satellite laser ranging (Loomis et al., 2019). Due to high-frequency noise in high-degree/-order SHCs, a 300-km Gaussian filtering (Jekeli, 1981) is applied. Subsequently, the SHCs are transformed into TWS changes considering the ellipsoid correction (Ditmar, 2018; Li et al., 2017).

3. Method

In line with Ditmar et al. (2018) and Ditmar (2022), this study explores the application of VCE (Koch & Kusche, 2002; Kusche, 2003) and regularization to enhance the combination of various TWS change time series

at specific geographic locations into a single time series, addressing the challenges of nonstationary signals. To minimize the suppression of seasonal signals, we consider five regularization functionals. Three of them minimize the unknown function itself or its derivatives known as zero-order, first-order, and second-order Tikhonov regularization (Tikhonov, 1977), abbreviated as Tikh-0, Tikh-1, and Tikh-2, respectively. The remaining two regularization functionals, designed by Ditmar et al. (2018) and Ditmar (2022), penalize month-to-month year-to-year double differences (MYDD) and month-to-month year-to-year triple differences (MYTD) of TWS changes, allowing signals related to climate stationarity, such as signals of annual periodicity and linear trends, to escape penalization. Additionally, the individual TWS time series are also combined using VCE without applying any regularization, referred to as "no-reg." By minimizing the following objective function, we combine various TWS change time series at a specific grid point as follows:

$$\Phi(x) = \frac{1}{\sigma_1^2}\sum_i \left(x_i - d_i^1\right)^2 + \cdots + \frac{1}{\sigma_k^2}\sum_i \left(x_i - d_i^k\right)^2 + \cdots + \frac{1}{\sigma_n^2}\sum_i \left(x_i - d_i^n\right)^2 + \frac{1}{\sigma_x^2}\Omega(x), \tag{1}$$

where d_i^k represents TWS change in the i-th month derived from the k-th input mass anomaly time series, n is the number of analyzed mass anomaly time series, $\sigma_k^2 (k = 1, \cdots n)$ is the unknown error variance of the k-th input mass anomaly time series with σ_k being the standard deviation of the corresponding error, σ_x^2 is the unknown signal variance dependent on the regularization functional $\Omega(x)$, and $x_i (i = 1, 2, \cdots)$ is the combined time series to be estimated. More details could be found in Text S1 in Supporting Information S1.

4. Results

4.1. Estimation of Noise Levels of Individual GRACE Solutions by VCE

As mentioned in Section 3, VCE was applied to determine the weights applied to GRACE solutions from different processing centers. These weights originate from the estimated noise levels of the GRACE solutions. Therefore, the noise level of each individual GRACE solution determines how that solution contributes to the final combination solution. Figure 1 shows the noise levels for all the considered GRACE solutions represented as standard deviations estimated by VCE in the combination with Tikh-2 regularization. Figure 1a demonstrates the global maps of noise level estimates which reveal a remarkable dependency on geographic latitude: noise is relatively high near the equator and gradually decreases toward the poles. This can be attributed to variations in the density of GRACE observation points and observation geometry.

Apart from a similar dependency on the latitude, some of the solutions demonstrate different error patterns in specific regions. For CSR solutions, the noise levels increase in Foxe Basin, the northwest coast of Australia, and the Filchner-Ronne Ice Shelf (red circles/ovals in Figure 1a), compared to the surrounding areas, which is consistent with the findings of Ditmar (2022). These features are probably related to the 161-day S2 tide signal (Kvas et al., 2019).

For the HUST solutions, regions located in the Sea of Japan, Andaman Sea, and the Gulf of Carpentaria (red ovals in Figure 1a) exhibit increased noise levels. This may be related to the usage of the new background model (AOD1B RL07) which is incorporated exclusively in the processing strategy of the HUST solutions. At the same time, the HUST solutions here have been significantly improved compared to HUST-Grace2016 in Ditmar (2022), where they underperformed compared to other solutions. After the upgrade, the HUST solutions now demonstrate a performance comparable to CSR and ITSG solutions. The characteristics of noise levels of JPL, GFZ, and WHU solutions remain consistent with the findings in the study of Ditmar (2022). Figures 1b and 1c shows box plot of standard deviation over ocean and land respectively for each GRACE solution. The median standard deviation values shown in box plot quantitatively evaluate accuracy of each GRACE solution. The results indicate that each model has the same level of error both over the ocean and land, which directly confirms the assumption in Chen et al. (2021) that the error levels over the ocean and land are the same. By comparing the median standard deviations of different models, we can clearly see that the accuracy of CSR, ITSG, and HUST is the best among the models used, followed by WHU, JPL, and GFZ, respectively. These median standard deviation values also facilitate a direct comparison with the median value shown in Figure 2b and Figure S2 in Supporting Information S1. The estimation of noise levels in combination with other regularization functionals and without a regularization yields similar patterns to those observed in the case of Tikh-2 regularization (Figures S3–S7 in Supporting Information S1).

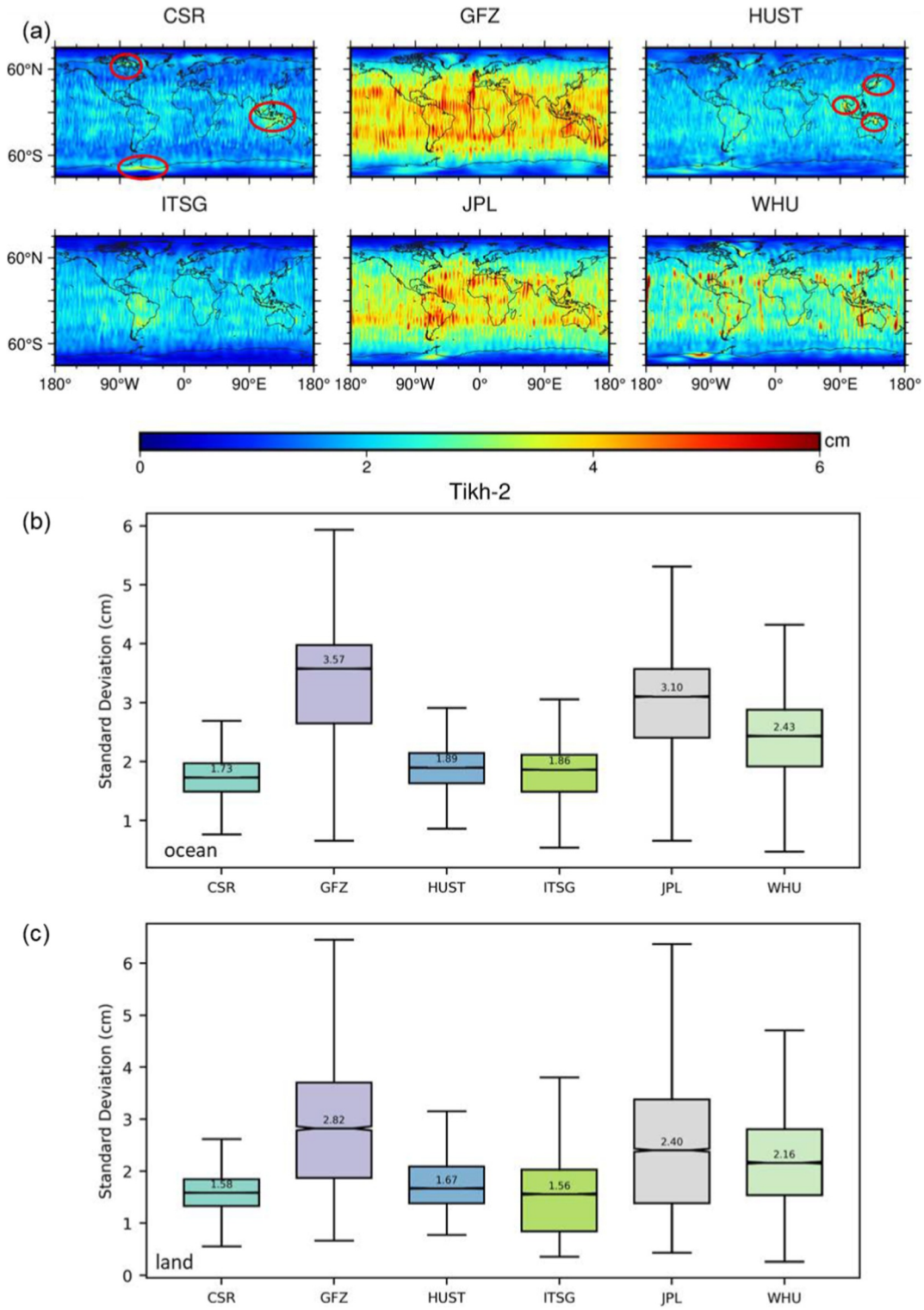

Figure 1. Standard deviations of TWS changes based on GRACE solutions from different data processing centers. The estimates are obtained by VCE with Tikh-2 regularization. (a) Spatial distribution of standard deviation of GRACE solutions. (b) Box plot of oceanic standard deviation for each GRACE solution. (c) Box plot of terrestrial standard deviation for each GRACE solution.

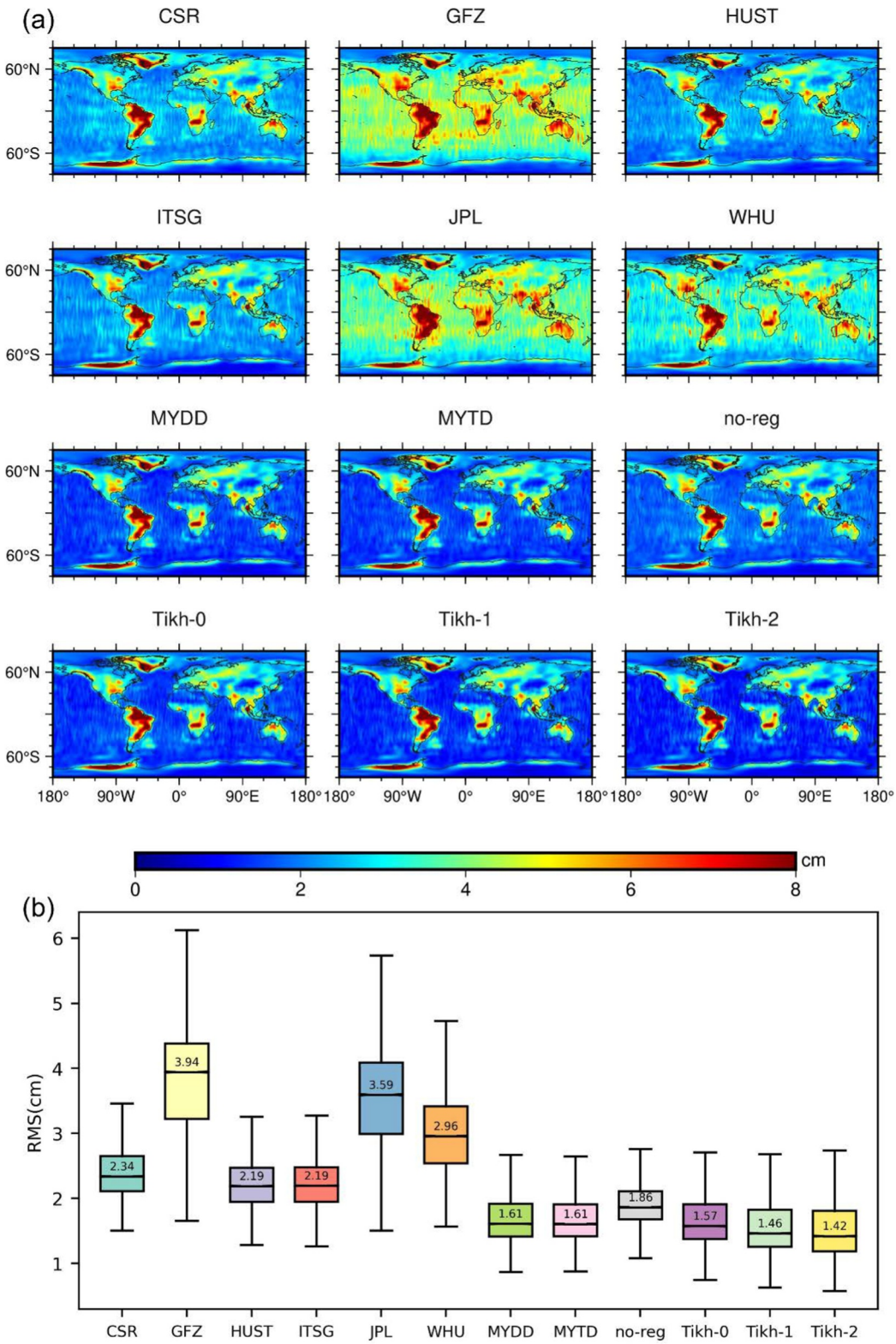

Figure 2. Post-fit RMS residuals based on the adopted signal model. The residuals are obtained both for individual and combined GRACE solutions. (a) Global distribution of post-fit RMS residuals for each GRACE monthly solution time-series; (b) Boxplot of oceanic post-fit RMS residuals for each GRACE monthly solution time-series.

4.2. Noise Assessment for Combined and Individual Solutions

To validate the reasonableness of the solution noise levels estimated by the VCE method, an independent accuracy assessment approach was introduced. We fitted a signal model to different combined and individual solutions. This signal model consists of the bias, trend, as well as semi-annual and annual periodic components. After the removal of signal model from mass variations, post-fit root mean square (RMS) residuals were calculated to evaluate the accuracy of GRACE solutions (Chen et al., 2021; Meyer et al., 2019; Zhong et al., 2023).

Figure 2a shows the post-fit RMS residuals of monthly GRACE solution time-series as global maps. Over the land, the residuals display large magnitudes, likely due to the presence of signals not captured by the signal model. In contrast, over oceans, where mass variations are minimal and well-absorbed by the signal model, the residuals are regarded as standard deviation of the errors contained in the analyzed data to a large extent. Thus, post-fit RMS residuals over oceans could serve as a measure of GRACE solution accuracy. Figure 2b shows the median oceanic post-fit RMS residual values as box plots. At the same time, the median terrestrial post-fit RMS residual values are illustrated in Figure S2 in Supporting Information S1. Despite regional variations, the median post-fit RMS residuals over land are comparable to those over the ocean, even though the terrestrial domain shows larger residuals in the global map. The finding suggests that the error levels are the same both over land and ocean.

Up to this point, we have employed two methods to evaluate the accuracy of individual solutions. The first method, described in subsection 4.1, uses VCE, while in this subsection, we assess accuracy by examining the difference between the signal model and the data time-series. Both approaches yield nearly consistent results. As shown in Figures 1b and 2b, the median oceanic post-fit RMS residuals for HUST, CSR, and ITSG solutions are comparable. WHU solutions show a somewhat higher uncertainty, but outperform JPL and GFZ solutions. The relative pattern of noise levels among these solutions, based on the difference between the original data time-series and modeled signals, align with those derived through VCE. This confirms the reliability of our accuracy assessment.

Furthermore, comparing the accuracies of the combined and individual solutions provides preliminary evidence supporting the assumption of this study: a combination of solutions increases the accuracy, whereas the addition of a regularization could reduce the RMS residuals further, compared to the combined solution obtained without a regularization. Statistical calculations show that the highest accuracy (i.e., the lowest value of median oceanic post-fit RMS residuals) of the individual solutions is 2.19 cm (Figure 2b). Meanwhile, the accuracy of the unregularized combined solutions is 1.86 cm, whereas the average accuracy of the regularized combined solutions reaches 1.53 cm. Compared to the highest accuracy of the individual solutions, the unregularized combined solution improves the mass anomaly estimation by 15%, while the regularized combined solutions show an RMS residual reduction of ∼30%. Meanwhile, compared to the unregularized combined solution, the average accuracy improvement provided by a regularization is ∼18%. Notably, the combined solutions obtained with Tikh-2 regularization show the relative higher accuracy compared to the other regularized combined solutions in terms of the median of oceanic post-fit RMS residuals.

4.3. Signal Comparison of GRACE Solutions

Since evaluating only the noise levels of the solutions do not provide a comprehensive understanding of their overall performance, we compare the signal content of individual and combined GRACE solutions over several regions, that is, basins of Amazon, Yangtze River, and Yellow River as well as Greenland and Aral Sea. In the first instance, TWS variations within a basin are averaged across the basin grid cells, with each cell weighted by the sine of its colatitude. The acquired TWS time series is then transformed into amplitude spectral density (ASD), so that we can analyze the amplitude of TWS time series at a specific frequency band (Bonin et al., 2012). Figure 3 compares the ASD of TWS time series in the Yellow River basin. Meanwhile, the basin-scale TWS time series of each GRACE solution in Yellow River are shown in Figure S8 in Supporting Information S1 and the signal components extracted from TWS time series in Yellow River are illustrated in Figure S9 in Supporting Information S1. The 1 cpy (cycles per year) and 2 cpy ASD correspond to the annual and semi-annual amplitudes, respectively. At the same time, their magnitudes are closely comparable. This demonstrates the effectiveness of the Fourier transform in extracting the energy of signals at different frequencies. Furthermore, the signal components (long-term trend, annual amplitude and semi-annual amplitude) of the regularization combination solution are at a same level to those of the COST-G (Combination Service for Time-variable Gravity Fields)

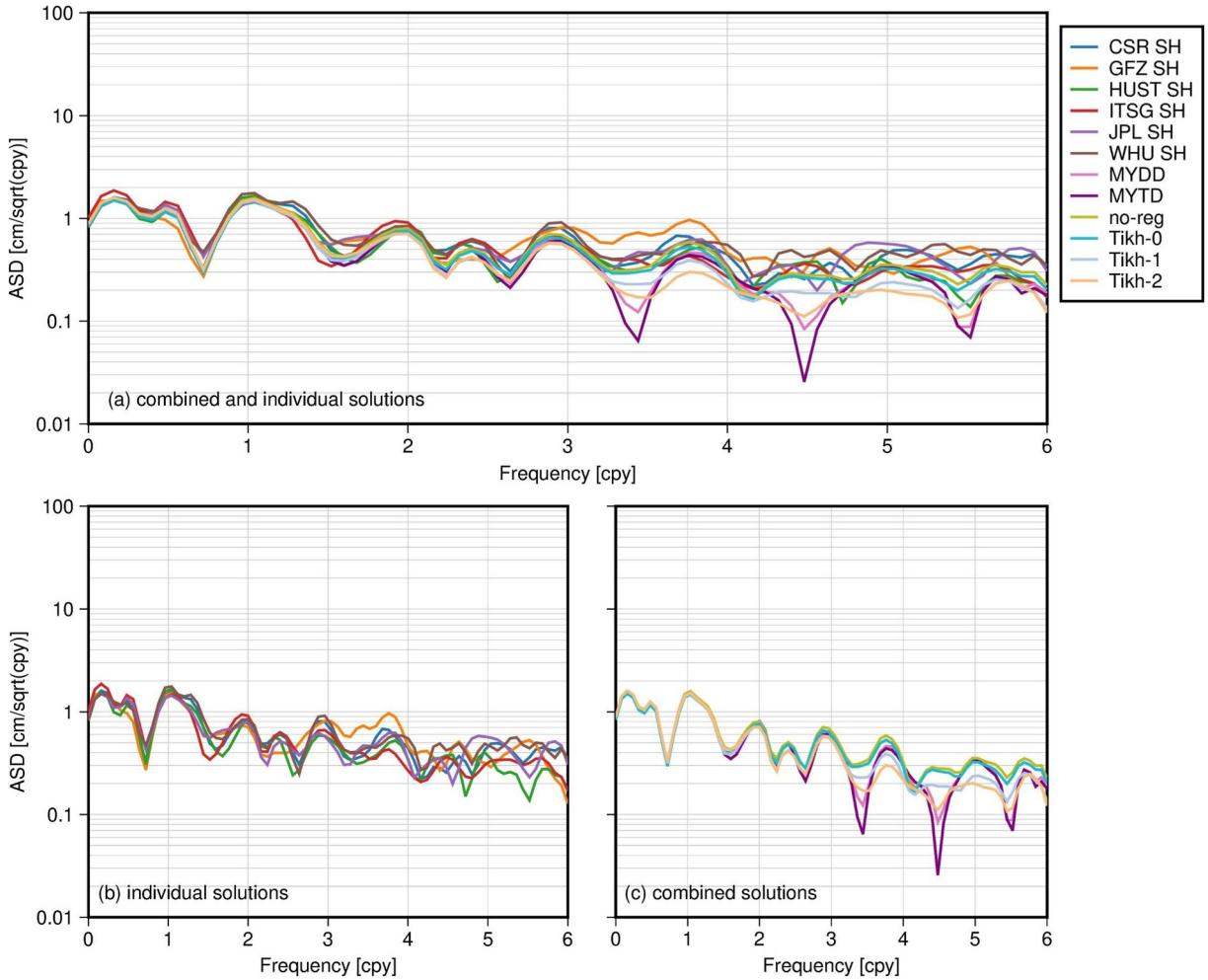

Figure 3. TWS variations of GRACE solutions in Yellow River basin. (a) TWS variations of combined and individual solutions in spectral domain. (b) TWS variations of individual solutions in spectral domain. (c) TWS variations of combined solutions in spectral domain.

solution. This indicates that the effective signals are well preserved in the combination solutions. When analyzing the TWS time series of GRACE solutions in time domain (Figures S8, S10–S13 in Supporting Information S1), the discrepancies between regularized combined solutions and individual solutions can hardly be observed, which alludes to the fact that the combined models contain almost the same signals as the individual models. In the spectral domain, the amplitudes of GRACE combined solutions at frequencies below 3 cpy present negligible discrepancies, which suggests that the long-term trends, annual and semi-annual signals of the various models are generally consistent. But compared to individual solutions, the regularized combined solutions exhibit notable energy loss in high-frequency bands above 3 cpy. In particular, the solution with MYTD regularization, which is designed to preserve signals recurring in the same month of neighboring years while suppressing signals from occasional events, shows significant amplitude attenuation at non-integer frequency bands.

TWS variations of GRACE solutions in other regions are shown in Figures S8, S10–S13 in Supporting Information S1. Except for the Amazon basin, where discrepancies between individual and combined solutions are negligible across all frequency ranges, noticeable energy loss is observed in the combined solution with MYTD regularization at high-frequency bands, particularly at non-integer frequency bands, in the Yangtze River basin, Greenland, and Aral Sea. The amplitude attenuation occurs in the high-frequency bands, which is most likely due to noise suppression. However, the possibility that some of this loss results from the suppression of signals associated with short-term events (e.g., flood and drought) cannot be completely ruled out. Therefore, we applied both individual and combined GRACE TWS solutions to identify drought events around the Yangtze River Basin (Tables S3 and S4 in Supporting Information S1), and compared the drought events derived from the combined

solutions with those from the individual solutions. The results show that the drought events identified by individual solutions are also captured by the combined models. Moreover, the drought events identified from the GRACE solutions are also recorded in the EM-DAT Emergency Events Database (Table S5 in Supporting Information S1). This suggests that while model combination may suppress certain high-frequency signals (which could be high-frequency noise), it does not suppress valid short-term hydrological signals.

In addition, we compared the regularization combination solutions with the COST-G and the CSR Mascon (CSR MC) across multiple basins (Table S6, Figure S14–S33 in Supporting Information S1). The results show that in the Indus, Ganges, Zambezi, Amur, and Niger basins, the regularization combination solutions exhibit smaller amplitudes compared to CSR MC but approximate the amplitudes of COST-G. This is due to signal leakage resulting from the absence of leakage error corrections in the SHC solutions. Meanwhile, in the Yellow River, Yangtze, Orange, and Murray basins, the regularization combination solution demonstrates lower noise compared to COST-G in certain periods and aligns more closely with CSR MC. Through comparison with COST-G and CSR MC, it is evident that the effective signals in the regularization combination solution of this study are well preserved, while anomalous fluctuations have been effectively removed.

4.4. Comparison With Altimetry-Derived Caspian Sea Level Changes

To further investigate the signal characteristics of each GRACE solution, we compared the GRACE-derived signals with altimetry observations. Significant water mass variations in the Caspian Sea can be easily monitored by GRACE, with minimal interference from arid areas east to the Caspian Sea—an ideal condition for isolating water level change signals. Additionally, satellite altimetry, an independent geodetic technique, can effectively monitor these water level changes, providing a valuable method to validate GRACE solutions (Chen et al., 2017; Swenson & Wahr, 2007). Extracting Caspian Sea Level (CSL) changes from GRACE data requires a post-processing of the GRACE-derived TWS changes. This includes correcting for outward signal leakage using constrained forward modeling (Chen et al., 2014), where a scale factor of 1/F ($F = 0.4$) is estimated in practice. More details of forward modeling are shown in Figure S1 in Supporting Information S1. To mitigate the inward signal leakage, a hydrological model (GLDAS-noah (https://hydro1.gesdisc.eosdis.nasa.gov/data/GLDAS/GLDAS_NOAH10_M.2.1/)) describing TWS variations around the Caspian Sea has to be used. Steric sea level variations driven by temperature and salinity changes (https://hadleyserver.metoffice.gov.uk/en4/download.html) should also be accounted for. Figure 4a shows comparison of CSL changes derived from individual and combined GRACE solutions with CSL changes from satellite altimetry (https://hydroweb.next.theia-land.fr/). Compared to satellite altimetry observations, the GRACE data show variations of a similar magnitude. However, the time series derived from individual solutions show stronger noise than those from the combined solutions, highlighting the noise reduction and enhanced signal-to-noise ratio achieved through solution combination. Figure 4b shows the ASD of GRACE-derived and altimetry-derived CSL change time series. One dominant peak with highest energy levels is observed at 1 cpy. Furthermore, there is an order of magnitude drop between 1 and 2 cpy and the energy of CSL signal keeps decreasing from 2 to 6 cpy, indicating that the interannual and annual signals are the primary components of CSL changes. In addition, compared to the individual and non-regularized combined solutions, regularized combined solutions exhibit consistent amplitude between 0 and 2 cpy. At the same time, all GRACE-derived CSL changes keep consistent energy levels with altimetry-derived CSL changes within frequency range below 2 cpy. Within the frequency range above 2 cpy, the amplitude discrepancies among individual GRACE solutions increase with frequency, while the amplitudes of the regularized combined solutions are consistent with those of the non-regularized ones. However, a little energy loss of regularized solutions is present, especially between 5 and 6 cpy, which may be attributed to either noise reduction or signal attenuation attributed to the regularization schemes.

According to Equation 1 shown in Ditmar (2022), we have estimated the scaling coefficient for each GRACE solution to measure the signal damping in the regularized combined solutions. This damping is quantified as a scaling coefficient defined as the ratio of CSL changes estimated from GRACE solutions to those observed by satellite altimetry. A larger value indicates a stronger signal retaining in the GRACE solutions. As shown in Figure S34 in Supporting Information S1, the scaling coefficient values of most GRACE solutions are in the range of 0.4–0.41, which is consistent with the value ($F = 0.400$) estimated by constrained forward modeling. The regularized combined solutions appear no signal damping compared to the non-regularized ones. These results suggest that the method employed to assess signal retention in GRACE solutions is effective, and that signal damping caused by regularization is barely evident over the Caspian Sea.

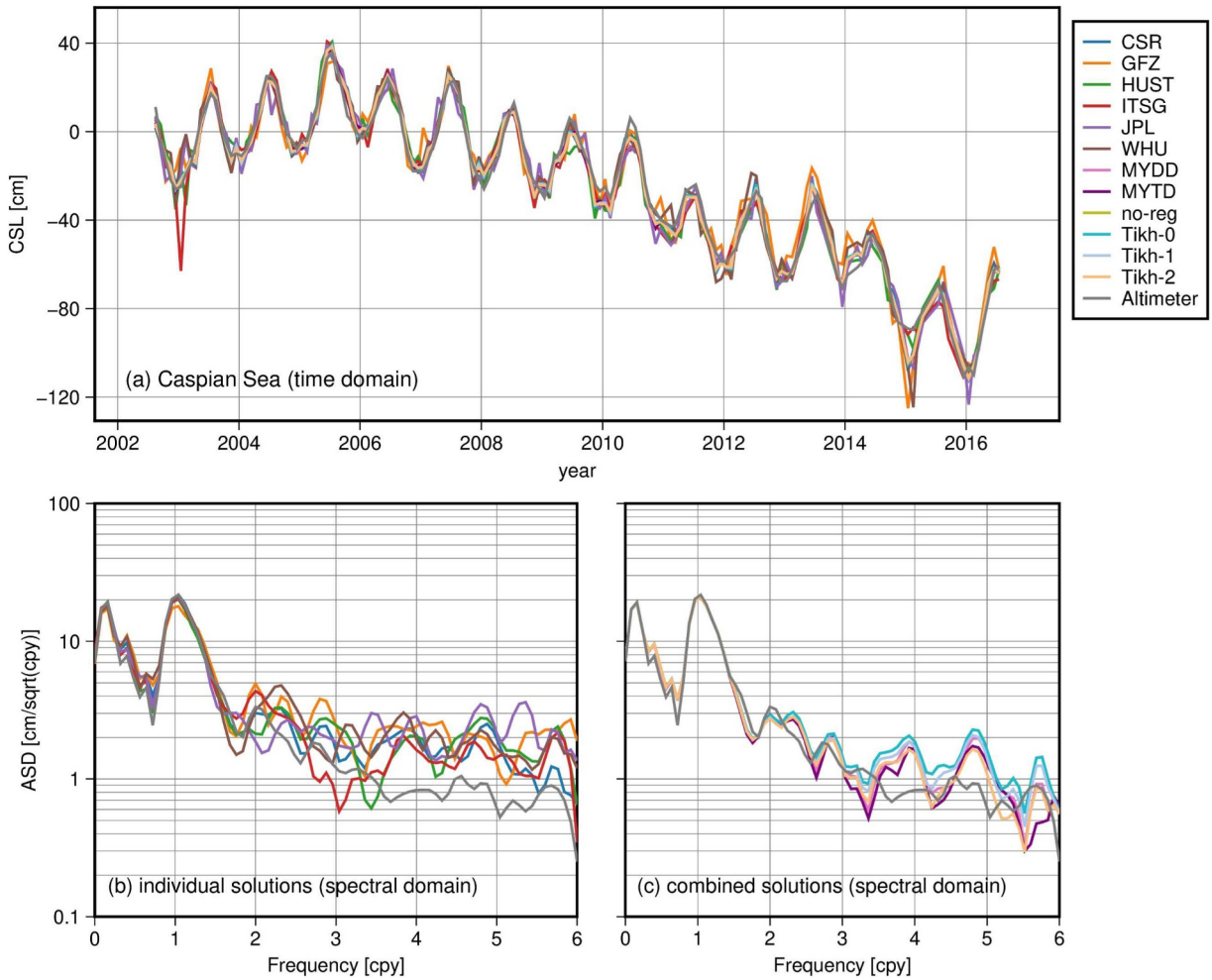

Figure 4. Comparison between altimetry-based and gravimetry-based CSL changes. (a) CSL changes time series derived from GRACE solutions and satellite altimetry observation. (b) and (c) The amplitude spectral density of GRACE-derived and altimetry-derived CSL change time series.

At the same time, we have calculated statistical metrics, including Pearson correlation coefficient (PCC), Nash-Sutcliffe efficiency (NSE), and normalized root-mean-square error (NRMSE) (Table S2 in Supporting Information S1), to assess the alignment between GRACE solutions and satellite altimetry observations (Moriasi et al., 2007). The results indicate that higher correlations occur in the case of combined GRACE solutions, particularly with Tikh-2 regularization, as compared to the individual ones. Those combined solutions outperform the individual solutions by 0.9% in PCC, 1.9% in NSE, and 1.3% in NRMSE on average, while the Tikh-2 regularization also holding a slight advantage over other combined solutions. These findings confirm that the regularized combined solutions, matching or even surpassing individual solutions, align well with independent satellite altimetry observations, further supporting the usage of regularization.

5. Conclusions

In this study, we merged TWS changes derived from GRACE SHC solutions produced at different data processing centers (i.e., CSR, GFZ, HUST, ITSG, JPL, and WHU) to generate combined global TWS solutions from August 2002 to July 2016, while introducing various regularization constraints into combination process: Tikh-0, Tikh-1, Tikh-2, MYDD, and MYTD. The relative weights of individual TWS estimates and regularization parameters were adaptively determined using VCE. Through VCE, not only was the TWS fusion completed, but also the accuracy of TWS estimates from individual GRACE solutions could be estimated (Ditmar, 2022). The relative accuracy patterns of individual solutions revealed by the VCE method were compared over the ocean with those obtained from an independent accuracy evaluation method based on post-fit residuals after removing the

signal model of TWS changes. Only slight discrepancies in the accuracy assessments between the two methods were revealed. This consistency confirms the reliability of the accuracy evaluation results and weighting schemes in this study.

To assess the performance of the regularized combined TWS solutions, we compared them with individual GRACE TWS solutions and unregularized combined TWS solutions in terms of noise levels and signal damping. In terms of noise levels, the combined solutions with regularization demonstrated a larger noise reduction compared to those without regularization, with an average improvement of 18%. Among the regularized solutions, the Tikh-2 solutions showed a slight advantage over other regularized solutions. Additionally, the results suggested that the noise level in novel HUST-Grace2024 data product has reached the same level as in CSR and ITSG solutions. Regarding the signal content, basin-scale TWS variations were calculated for each GRACE solution over several regions: Amazon, Greenland, Aral Sea, Yellow River, and Yangtze River. For a detailed analysis, the TWS change time series of GRACE solutions are presented and compared in both time and spectral domains. When analyzing in time domain, only minor discrepancies were exhibited between individual and combined solutions. However, after the TWS variations were transformed into spectral domain, energy loss of TWS variations triggered by regularization was evident at high-frequency bands. In particular, the MYTD regularization caused the most evident amplitude attenuation among all of regularization methods at non-integer frequencies (in terms of cpy). In addition, the drought events detected by individual solutions can also be monitored by the combined solutions, indicating that effective short-term hydrological signals are preserved after model combination. Furthermore, from the comparison results between the regularized combination solutions, COST-G, and CSR Mascon, it can be observed that the regularized combination solution exhibits a similar level of signal strength as COST-G, while demonstrating less disturbed signals during certain periods (Figures S14–S33 in Supporting Information S1). These demonstrate that the model combination process effectively preserves valid and realistic geophysical signals.

Additionally, mass anomalies in the Caspian Sea were considered. GRACE-derived CSL changes were compared to CSL changes from altimetry observations to assess the signal retaining of each GRACE solution. In time domain, there are only minor differences between GRACE-based and altimetry-based CSL change time series, for example, the PCC, NSE, and NRSE between ITSG and altimetry is 0.9861, 0.9699, and 0.0387 respectively. In spectral domain, the amplitudes of GRACE-based CSL variations are consistent with that of altimetry-based ones at the frequencies up to 2 cpy. At frequencies above 2 cpy, individual GRACE solutions present more diverse amplitudes and stronger power than combined GRACE solutions. However, compared to altimetry observations, this stronger power may be attributed to the effect of noise. Furthermore, we have calculated the scaling coefficient for each GRACE solution to assess the signal retaining of GRACE solutions related to altimetry observations. The scaling coefficients of most GRACE solutions fall within the range of 0.40–0.41. The results suggested that the regularized combined solutions contain comparable signal levels with individual and non-regularized combined solutions over the Caspian Sea. Therefore, we can presume that the energy loss triggered by regularization at high-frequency bands may be categorized as noise reduction. In addition, the difference between the regularized solutions and satellite altimetry observations shows slightly better performance than that of individual solutions, validating the reliability of the regularized approach.

Combining solutions is a practical approach to mitigate inaccuracies specific for different GRACE data processing strategies. This study, for the first time, incorporates regularization constraints into TWS combination to estimate more accurately TWS changes. Compared to unconstrained combinations, regularized solutions further reduce noise. The second-order Tikhonov regularization ("Tikh-2") slightly outperforms other regularization types in terms of noise reduction. On the other hand, the introduction of regularization leads to energy loss at high-frequency bands, particularly in the case of the MYTD regularization. Future research could delve into whether the optimal choice of regularization depends on the signal of interest, taking into account different climatic conditions of the study regions. However, the current method is purely constructed based on the temporal properties of the models, and thus inherently overlooks their spatial structural features. How to consider the spatial and temporal properties of models simultaneously will be the focus of our subsequent work.

Conflict of Interest

The authors declare no conflicts of interest relevant to this study.

Availability Statement

All the temporal gravity field models used in this study are publicly available at https://icgem.gfz-potsdam.de/sl/temporal. The GLDAS model used in this study is from https://hydro1.gesdisc.eosdis.nasa.gov/data/GLDAS/GLDAS_NOAH10_M.2.1/. Steric sea level variations of CSL are publicly available at https://hadleyserver.metoffice.gov.uk/en4/download.html. The CSL altimetry data is publicly available at https://hydroweb.next.theia-land.fr/.

Acknowledgments
This work was funded by the National Natural Science Foundation of China (42474005, 42174014).

References

Bettadpur, S. (2018). *Gravity recovery and climate experiment level-2 gravity field product user handbook*. Center for Space Research at The University of Texas at Austin. Retrieved from https://archive.podaac.earthdata.nasa.gov/podaac-ops-cumulus-docs/grace/open/docs/L2-UserHandbook_v4.0.pdf

Bonin, J. A., Bettadpur, S., & Tapley, B. D. (2012). High-frequency signal and noise estimates of CSR GRACE RL04. *Journal of Geodesy*, *86*(12), 1165–1177. https://doi.org/10.1007/S00190-012-0572-5

Chen, J., Li, J., Zhang, Z., & Ni, S. (2014). Long-term groundwater variations in Northwest India from satellite gravity measurements. *Global and Planetary Change*, *116*, 130–138. https://doi.org/10.1016/J.GLOPLACHA.2014.02.007

Chen, J., Tapley, B., Tamisiea, M. E., Save, H., Wilson, C., Bettadpur, S., & Seo, K.-W. (2021). Error assessment of GRACE and GRACE Follow-On mass change. *Journal of Geophysical Research: Solid Earth*, *126*(9), e2021JB022124. https://doi.org/10.1029/2021JB022124

Chen, J. L., Wilson, C. R., Tapley, B. D., Save, H., & Cretaux, J. F. (2017). Long-term and seasonal Caspian Sea level change from satellite gravity and altimeter measurements. *Journal of Geophysical Research: Solid Earth*, *122*(3), 2274–2290. https://doi.org/10.1002/2016JB013595

Dahle, C., Murböck, M., Flechtner, F., Dobslaw, H., Michalak, G., Neumayer, K., et al. (2019). The GFZ GRACE RL06 monthly gravity field time series: Processing details and quality assessment. *Remote Sensing*, *11*(18), 2116. https://doi.org/10.3390/rs11182116

Ditmar, P. (2018). Conversion of time-varying Stokes coefficients into mass anomalies at the Earth's surface considering the Earth's oblateness. *Journal of Geodesy*, *92*(12), 1401–1412. https://doi.org/10.1007/S00190-018-1128-0

Ditmar, P. (2022). How to quantify the accuracy of mass anomaly time-series based on GRACE data in the absence of knowledge about true signal? *Journal of Geodesy*, *96*(8), 54. https://doi.org/10.1007/S00190-022-01640-X

Ditmar, P., Tangdamrongsub, N., Ran, J., & Klees, R. (2018). Estimation and reduction of random noise in mass anomaly time-series from satellite gravity data by minimization of month-to-month year-to-year double differences. *Journal of Geodynamics*, *119*, 9–22. https://doi.org/10.1016/j.jog.2018.05.003

Gao, S., Hao, W., Fan, Y., Li, F., & Wang, J. (2023). A multi-source GRACE fusion solution via uncertainty quantification of GRACE-Derived terrestrial water storage (TWS) change. *Journal of Geophysical Research: Solid Earth*, *128*(11), e2023JB026908. https://doi.org/10.1029/2023jb026908

Jean, Y., Meyer, U., & Jäggi, A. (2018). Combination of GRACE monthly gravity field solutions from different processing strategies. *Journal of Geodesy*, *92*(11), 1313–1328. https://doi.org/10.1007/s00190-018-1123-5

Jekeli, C. (1981). Alternative methods to smooth the Earth's gravity field.

Koch, K.-R., & Kusche, J. (2002). Regularization of geopotential determination from satellite data by variance components. *Journal of Geodesy*, *76*(5), 259–268. https://doi.org/10.1007/s00190-002-0245-x

Kusche, J. (2003). A Monte-Carlo technique for weight estimation in satellite geodesy. *Journal of Geodesy*, *76*(11–12), 641–652. https://doi.org/10.1007/s00190-002-0302-5

Kusche, J. (2007). Approximate decorrelation and non-isotropic smoothing of time-variable GRACE-type gravity field models. *Journal of Geodesy*, *81*(11), 733–749. https://doi.org/10.1007/S00190-007-0143-3

Kusche, J., Schmidt, R., Petrovic, S., & Rietbroek, R. (2009). Decorrelated GRACE time-variable gravity solutions by GFZ, and their validation using a hydrological model. *Journal of Geodesy*, *83*(10), 903–913. https://doi.org/10.1007/S00190-009-0308-3

Kvas, A., Behzadpour, S., Ellmer, M., Klinger, B., Strasser, S., Zehentner, N., & Mayer-G U Rr, T. (2019). ITSG-Grace2018: Overview and evaluation of a new GRACE-only gravity field time series. *Journal of Geophysical Research: Solid Earth*, *124*(8), 9332–9344. https://doi.org/10.1029/2019JB017415

Landerer, F. W., Flechtner, F. M., Save, H., Webb, F. H., Bandikova, T., Bertiger, W. I., et al. (2020). Extending the global mass change data record: GRACE follow-on instrument and science data performance. *Geophysical Research Letters*, *47*(12), e2020GL088306. https://doi.org/10.1029/2020GL088306

Li, J., Chen, J., Li, Z., Wang, S. Y., & Hu, X. (2017). Ellipsoidal correction in GRACE surface mass change estimation. *Journal of Geophysical Research: Solid Earth*, *122*(11), 9437–9460. https://doi.org/10.1002/2017jb014033

Loomis, B. D., Rachlin, K. E., & Luthcke, S. B. (2019). Improved Earth oblateness rate reveals increased ice sheet losses and mass-driven sea level rise. *Geophysical Research Letters*, *46*(12), 6910–6917. https://doi.org/10.1029/2019GL082929

Meyer, U., Jean, Y., Kvas, A., Dahle, C., Lemoine, J. M., & Jäggi, A. (2019). Combination of GRACE monthly gravity fields on the normal equation level. *Journal of Geodesy*, *93*(9), 1645–1658. https://doi.org/10.1007/S00190-019-01274-6

Meyer, U., Lasser, M., Dahle, C., Förste, C., Behzadpour, S., Koch, I., & Jäggi, A. (2023). Combined monthly GRACE-FO gravity fields for a global gravity-based groundwater product. *Geophysical Journal International*, *236*(1), 456–469. https://doi.org/10.1093/gji/ggad437

Moriasi, D. N., Arnold, J. G., Van Liew, M. W., Bingner, R. L., Harmel, R. D., & Veith, T. L. (2007). Model evaluation guidelines for systematic quantification of accuracy in watershed simulations. *Transactions of the ASABE*, *50*(3), 885–900. https://doi.org/10.13031/2013.23153

Mu, D., Yan, H., Feng, W., & Peng, P. (2017). GRACE leakage error correction with regularization technique: Case studies in Greenland and Antarctica. *Geophysical Journal International*, *208*(3), 1775–1786. https://doi.org/10.1093/GJI/GGW494

Prevost, P., Chanard, K., Fleitout, L., Calais, E., Walwer, D., Van Dam, T., & Ghil, M. (2019). Data-adaptive spatio-temporal filtering of GRACE data. *Geophysical Journal International*, *219*(3), 2034–2055. https://doi.org/10.1093/GJI/GGZ409

Sakumura, C., Bettadpur, S., & Bruinsma, S. (2014). Ensemble prediction and intercomparison analysis of GRACE time-variable gravity field models. *Geophysical Research Letters*, *41*(5), 1389–1397. https://doi.org/10.1002/2013gl058632

Sun, Y., Riva, R., & Ditmar, P. (2016). Optimizing estimates of annual variations and trends in geocenter motion and J2 from a combination of GRACE data and geophysical models. *Journal of Geophysical Research: Solid Earth*, *121*(11), 8352–8370. https://doi.org/10.1002/2016JB013073

Swenson, S., & Wahr, J. (2006). Post-processing removal of correlated errors in GRACE data. *Geophysical Research Letters*, *33*(8). https://doi.org/10.1029/2005GL025285

Swenson, S., & Wahr, J. (2007). Multi-sensor analysis of water storage variations of the Caspian Sea. *Geophysical Research Letters*, *34*(16). https://doi.org/10.1029/2007gl030733

Tapley, B. D., Watkins, M. M., Flechtner, F., Reigber, C., Bettadpur, S., Rodell, M., et al. (2019). Contributions of GRACE to understanding climate change. *Nature Climate Change*, *9*(5), 358–369. https://doi.org/10.1038/S41558-019-0456-2

Tikhonov, A. N. (1977). *Solutions of Ill-posed problems*. VH Winston and Sons.

Yan, X., Zhang, B., Yao, Y., Yang, Y., Li, J., & Ran, Q. (2021). GRACE and land surface models reveal severe drought in eastern China in 2019. *Journal of Hydrology*, *601*, 126640. https://doi.org/10.1016/j.jhydrol.2021.126640

Yuan, D. (2018). *JPL level-2 processing standards document for level-2 product release 06*. Jet Propulsion Laboratory, California Institute of Technology.

Zhong, B., Li, X., Chen, J., & Li, Q. (2023). WHU-GRACE-GPD01s: A series of constrained monthly gravity field solutions derived from GRACE-based geopotential differences. *Earth and Space Science*, *10*(4), e2022EA002699. https://doi.org/10.1029/2022ea002699

Zhou, H., Zhou, Z., & Luo, Z. (2019). A new hybrid processing strategy to improve temporal gravity field solution. *Journal of Geophysical Research: Solid Earth*, *124*(8), 9415–9432. https://doi.org/10.1029/2019jb017752